

References

- [1] Battish, I., Hamad, A., and Mahani, R. Structure and dielectric studies of nano-composite Fe_2O_3 : BaTiO_3 prepared by sol-gel method. *Physica B* 404 (2009): 2274–2279.
- [2] Brzozowski, E. and Castro, M. Grain growth control in Nb-doped BaTiO_3 . *J. Mater. Process. Technol.* 168 (2005): 464–470.
- [3] Daoudi, K., Tsuchiya, T., and Kumagai, T. Pulsed-laser crystallization and epitaxial growth of metal-organic films of Ca-doped LaMnO_3 on STO and LSAT substrates. *Appl. Surf. Sci.* 253 (2007): 6527–6530.
- [4] Ye, Y. and Guo, T. Dielectric properties of Fe-doped $\text{Ba}_{0.65}\text{Sr}_{0.35}\text{TiO}_3$ thin films fabricated by the sol-gel method. *Ceram. Int.* 35 (2009): 2761–2765.
- [5] Sulaimana, M., Hutagalunga, S., Ainb, M., and Ahmada, Z. Dielectric properties of Nb-doped $\text{CaCu}_3\text{Ti}_4\text{O}_{12}$ electroceramics measured at high frequencies. *J. Alloys Compd.* 493 (2010): 486–492.
- [6] Chiodelli, G. et al. Electric and dielectric properties of pure and doped $\text{CaCu}_3\text{Ti}_4\text{O}_{12}$ perovskite materials. *Solid State Commun.* 132 (2004): 241–246.
- [7] Kundu, T., Jana, A., and Barik, P. Doped barium titanate nanoparticles. *Bull. Mater. Sci.* 31 (2008): 501–505.
- [8] Lina, F., Jianga, D., Maa, X., and Shi, W. Effect of annealing atmosphere on magnetism for Fe-doped BaTiO_3 ceramic. *Physica B* 403 (2008): 2525–2529.
- [9] Lin, F., Jiang, D., Ma, X., and Shi, W. Influence of doping concentration on room-temperature ferromagnetism for Fe-doped BaTiO_3 ceramics. *J. Magn. Magn. Mater.* 320 (2008): 691–691.

- [10] Hemer, S., Selmi, F., Varadan, V., and Varadan, V. The effect of various dopants on the dielectric properties of barium strontium titanate. *Mater. Lett.* 15 (1993): 317–324.
- [11] Gao, J., Zheng, L., Song, Z., Lin, C., and Zhu, D. γ ray irradiation effects of Au/PbTiO₃/YBa₂Cu₃O_{7- δ} capacitors under different bias voltage. *Mater. Lett.* 42 (2000): 345–349.
- [12] Arshak, K. et al. Properties of BGO thin films under the influence of gamma radiation. *Thin Solid Films* 516 (2008): 1493–1498.
- [13] Arshak, K. et al. Gamma Radiation Sensing Using ZnO and SnO₂ Thick Film Interdigitated Capacitors. *Electronics Technology, 2006. ISSE '06. 29th International Spring Seminar on* (2006): 483–488.
- [14] Ta, M., Briand, D., Boudart, B., and Guhel, Y. ⁶⁰Co gamma irradiation effects on electrical characteristics of Al/Y₂O₃/n-Si/Al capacitors. *Microelectron. Eng.* 87 (2010): 2158–2162.
- [15] Fasasi, A. et al. Thermoluminescence properties of barium titanate prepared by solid-state reaction. *Sens. Actuator A-Phys.* 135 (2007): 598–604.
- [16] Arshak, K. and Korostynska, O. Preliminary studies of properties of oxide thin/thick films for gamma radiation dosimetry. *Mater. Sci. Eng., B* 107 (2004): 224–232.
- [17] Ke, S., Huang, H., Fan, H., Chan, H., and Zhou, L. Structural and electric properties of barium strontium titanate based ceramic composite as a humidity sensor. *Solid State Ion.* 179 (2008): 1632–1635.
- [18] Zimmermann, F., Voigts, M., Menesklou, W., and Ivers-Tiffée, E. Ba_{0.6}Sr_{0.4}TiO₃ and BaZr_{0.3}Ti_{0.7}O₃ thick films as tunable microwave dielectrics. *J. Eur. Ceram. Soc.* 24 (2004): 1729–1733.

- [19] Kumar, A. and Manavalan, S. Characterization of barium strontium titanate thin films for tunable microwave and DRAM applications. *Surf. Coat. Technol.* 198 (2005): 406–413.
- [20] Li, W., Xu, Z., Chu, R., Fu, P., and Hao, J. Structure and electrical properties of BaTiO₃ prepared by sol-gel process. *J. Alloys Compd.* 482 (2009): 137–140.
- [21] Wang, X., Zhang, L., Liu, H., Zhai, J., and Yao, X. Dielectric nonlinear properties of BaTiO₃-CaTiO₃-SrTiO₃ ceramics near the solubility limit. *Mater. Chem. Phys.* 112 (2008): 675–678.
- [22] Xiao, C., Jin, C., and Wang, X. Crystal structure of dense nanocrystalline BaTiO₃ ceramics. *Mater. Chem. Phys.* 111 (2008): 209–212.
- [23] Jaffe, B., Cook, W., and Jaffe, H.. *Piezoelectric Ceramics*. Academic Press, London 1971.
- [24] Chen, K. and Chen, Y. Preparation of barium titanate ultrafine particles from rutile titania by a hydrothermal conversion. *Powder Technol.* 141 (2004): 69–74.
- [25] Maier, R. and Cohn, J. Ferroelectric and ferrimagnetic iron-doped thin-film BaTiO₃ : Influence of iron on physical properties. *J. Appl. Phys.* 92 (2002): 5429–5436.
- [26] Stashans, A. and Castillo, D. Simulation of iron impurity in BaTiO₃ crystals. *Physica B* 404 (2009): 1571–1575.
- [27] Onodera, A., Takesada, M., Kawatani, K., and Hiramatsu, S. Dielectric Properties and Phase Transition in CaCu₃Ti₄O₁₂ at High Temperatures. *J. Appl. Phys.* 47 (2008): 7753–7756.
- [28] Homes, C., Vogt, T., Shapiro, S., Wakimoto, S., and Ramirez, A. Optical Response of High-Dielectric-Constant Perovskite-Related Oxide. *Science* 293 (2001): 673–676.

- [29] Barber, P. et al. Polymer Composite and Nanocomposite Dielectric Materials for Pulse Power Energy Storage. *J. Mater. Sci. Technol.* 2 (2009): 1697–1733.
- [30] Fanga, L., Shen, M., and Cao, W. Effects of postanneal conditions on the dielectric properties of $\text{CaCu}_3\text{Ti}_4\text{O}_{12}$ thin films prepared on Pt/Ti/SiO₂/Si substrates. *J. Appl. Phys.* 95 (2004): 6483–6485.
- [31] Homes, C. et al. Charge transfer in the high dielectric constant materials $\text{CaCu}_3\text{Ti}_4\text{O}_{12}$ and $\text{CdCu}_3\text{Ti}_4\text{O}_{12}$. *Phys. Rev. B* 67 (2003): 092106(1)–092106(4).
- [32] Fiorenza, P. et al. Perovskite $\text{CaCu}_3\text{Ti}_4\text{O}_{12}$ thin films for capacitive applications: From the growth to the nanoscopic imaging of the permittivity. *J. Appl. Phys.* 105 (2009): 061634 – 061634–6.
- [33] Srivastava, A. et al. Dielectric relaxation in pulsed laser ablated $\text{CaCu}_3\text{Ti}_4\text{O}_{12}$ thin film. *J. Appl. Phys.* 100 (2006): 034102–034102–6.
- [34] Krohns, S. et al. Correlations of structural, magnetic, and dielectric properties of undoped and doped $\text{CaCu}_3\text{Ti}_4\text{O}_{12}$. *Eur. Phys. J. B* 72 (2009): 173–182.
- [35] Hernandez, M. et al. Eu-Doped BaTiO_3 Powder and Film from Sol-Gel Process with Polyvinylpyrrolidone Additive. *Int. J. Mol. Sci.* 10 (2009): 4088–4101.
- [36] Voll, D., Bera, A., and Schneider, H. Temperature-Dependent sol-gel-derived mullite spectroscopic study dehydration of precursors: an FTIR. *J. Eur. Ceram. Soc.* 18 (1998): 1101–1106.
- [37] Supasai, T. et al. Influence of temperature annealing on optical properties of $\text{SrTiO}_3/\text{BaTiO}_3$ multilayered films on indium tin oxide. *Appl. Surf. Sci.* 256 (2010): 4462–4467.
- [38] Kovacs, E. and Keresztesb, A. Effect of gamma and UV-B/C radiation on plant cells. *Micron* 33 (2002): 199–210.

- [39] Arshak, K. and Korostynska, O. Thin- and thick-film real-time gamma radiation detectors. *IEEE Sens. J.* 5 (2005): 574–580.
- [40] Shimoyama, K., Kubo, K., Maeda, T., and Yamabe, K. Epitaxial Growth of BaTiO₃ Thin Film on SrTiO₃ Substrate in Ultra High Vacuum without Introducing Oxidant. *J. Appl. Phys.* 40 (2001): L463–L464.
- [41] Caglar, M., Caglar, Y., and Ilcan, S. The determination of the thickness and optical constants of the ZnO crystalline thin film by using envelope method. *J. Optoelectron. Adv. Mater.* 8 (2006): 1410–1413.
- [42] Tauc, J. and Menth, A. States In The Gap. *J. Non-Cryst. Solids* 569 (1972): 8–10.
- [43] Elshabini, A. and Barlow, F.. *Thin films technology handbook..* New York 1998.
- [44] Serway, R. and Beichner, R.. *Physics for scientists and engineers with modern physics.* 5th ed. Philadelphia 2000.
- [45] Dejene, F. and Ocaya, R. lectrical, optical and structural properties of pure and gold-coated VO₂ thin films on quartz substrate. *Curr. Appl. Phys.* 10 (2010): 508–512.
- [46] Devan, R., Ma, Y., and Chougule, B. Effective dielectric and magnetic properties of (Ni-Co-Cu)ferrite/BTO composites. *Mater. Chem. Phys.* 115 (2009): 263–268.
- [47] Swanepoel, R. Determination of the thickness and optical constants of amorphous silicon. *J. Phys. E. Sci. Instrum.* 16 (1983): 1214–1222.
- [48] Mansingh, A. and Vasanta, C. Effect of the target on the structure and optical properties of radio-frequency sputtered barium titanate films. *J. Mater. Sci. Lett.* 7 (1988): 1104–1106.



- [49] Onton, A., Mareello, V., Lucovsky, G., and Galeener, F.. in *AIP Conf. Proc.* No. 31, AIP, New York, 1967.
- [50] Zhang, H. et al. Optical and electrical properties of sol-gel derived BaTiO₃ films on ITO coated glass. *Mater. Chem. Phys.* 63 (2000): 174–177.
- [51] Lu, X., Zhu, J., Zhang, W., Ma, G., and Wang, Y. The energy gap of r.f.-sputtered BaTiO₃ thin films with different grain size. *Thin Solid Films* 274 (1996): 165–168.
- [52] Burs, L. Electronic Wave Functions in Semiconductor Clusters: Experiment and Theory. *J. Phys. Chem.* 90 (1986): 2555–2560.
- [53] Nigro, R. et al. Calcium Copper-Titanate Thin Film Growth: Tailoring of the Operational Conditions through Nanocharacterization and Substrate Nature Effects. *J. Phys. Chem. B* 110 (2006): 17460–17467.
- [54] Kasa, Y.. *Microstructural and dielectric properties of calcium copper titanate thin films prepared by a sol-gel method.* Master's thesis Chulalongkorn University 2010.
- [55] A-Karmi, A. Impedance spectroscopy of gamma irradiated PM-355. *Radiat. Meas.* 41 (2006): 209–212.
- [56] Tataroglu, A. and Altndal, S. The effects of frequency and c-irradiation on the dielectric properties of MIS type Schottky diodes. *Nucl. Instrum. Methods Phys. Res. Sect. B-Beam Interact. Mater. Atoms* 254 (2007): 113–117.
- [57] A. Al-Karmi Impedance spectroscopy of gamma irradiated PM-355. *Radiat. Meas.* 41 (2006): 209–212.

APPENDICES

Appendix A

XRD database

The XRD peak position of barium titanate, calcium copper titanate, contamination substances (TiO_2 , CaTiO_3) thin films were confirmed by XRD database from The International Centre for Diffraction Data (ICDD) which shown as follows:

Pattern : 00-005-0826		Radiation = 1.540598		Quality : High		
BaTiO ₃		2th	i	h	k	l
Barium Titanium Oxide		22.039	12	0	0	1
		22.263	25	1	0	6
		31.498	100	1	0	1
		31.647	100	1	1	0
		36.656	48	1	1	1
		44.856	12	0	0	2
		45.376	37	2	0	0
		50.814	6	1	0	2
		50.978	6	2	0	1
		51.106	7	2	1	0
		55.255	15	1	1	2
		56.253	35	2	1	1
		65.755	12	2	0	2
		66.123	10	2	2	0
		70.359	6	2	1	2
		70.662	2	3	0	0
		74.336	5	1	0	3
		75.024	7	3	0	1
		75.164	9	3	1	0
Lattice : Tetragonal S.G. : P4mm (99) a = 3.99400 c = 4.03800 Z = 1		78.766	3	1	1	3
		79.472	5	3	1	1
		83.482	7	2	2	2
		86.565	1	2	0	3
		87.287	1	3	0	2
		88.049	1	3	2	0
		91.586	7	2	1	3
		92.060	12	3	1	2
		92.327	12	3	2	1
		96.494	1	0	0	4
		100.894	2	4	0	0
		103.669	1	1	0	4
		104.502	1	2	2	3
		104.991	1	3	2	2
		105.362	1	4	1	0
		106.256	3	1	1	4
		108.946	1	3	0	3
		109.732	6	4	1	1
		113.556	2	3	1	3
114.362	2	3	0	1		
117.506	3	2	0	4		
Color: Colorless Additional diffraction line(s): Plus 10 additional reflections Sample source or locality: Sample from National Lead Company. Sample preparation: Annealed at 1480 C in MgO. Analysis: Spectroscopic analysis: <0.1% Bi, Sr <0.01% Al, Ca, Fe, Mg, Pb, Si <0.001% Mn, Sn. General comments: Inverts to cubic form at 120 C. Temperature of data collection: X-ray pattern at 26 C. General comments: Merck Index, 8th Ed., p. 120. Data collection flag: Ambient						
Swanson, Fuyat, Natl. Bur. Stand. (U.S.), Circ. 539, volume 3, page 43, 1954. CAS Number: 12047-27-7						
Radiation : Cu-Ka1 Lambda : 1.54059 SS/FOM : F30= 19(0.0499,32)		Filter : Beta d-sp : Not given				

Pattern : 01-075-1149

Radiation = 1.540598

Quality : Alternate

CaCu₃Ti₄O₁₂

Calcium Copper Titanium Oxide

Also called: Calcium tricopper tetratitanium oxide

Lattice : Body-centered cubic

Mol. weight = 614.31

S.G. : Im-3m (229)

Volume [CD] = 404.08

a = 7.39300

Dx = 5.049

Z = 2

ν_{lcor} = 5.33

ICSD collection code: 030592

Test from ICSD: No R value given

Test from ICSD: At least one TF missing.

Cancel:

Data collection flag: Ambient

Deschanvres, A., Raveau, B., Tollemer, F., Bull. Soc. Chim. Fr., volume 1967, page 4077 (1967)

Calculated from ICSD using POWD-12++ (1997)

Radiation : CuKα1

Filter : Not specified

Lambda : 1.54060

d-sp : Calculated spacings

SS/FOM : F22=1000(0.0000,22)

2th	i	h	k	l
16.947	20	1	1	0
24.056	13	2	0	0
29.573	10	2	1	1
34.279	999	2	2	0
38.475	4	3	1	0
42.315	141	2	2	2
45.891	5	3	2	1
49.262	406	4	0	0
52.470	2	4	1	1
55.545	1	4	2	0
58.512	1	3	3	2
61.386	248	4	2	2
64.184	2	5	1	0
69.597	1	5	2	1
72.230	159	4	4	0
74.824	1	5	3	0
77.367	1	4	4	2
79.926	1	5	3	2
82.443	76	6	2	0
84.947	1	5	4	1
87.440	16	6	2	2
89.929	1	6	3	1

Pattern : 03-065-1156

Radiation = 1.540598

Quality : Deleted

TiO₂

Titanium Oxide

Lattice : Monoclinic

Mol. weight = 79.90

S.G. : P2₁/m (11)

Volume [CD] = 284.23

a = 12.17870

Dx = 1.867

b = 3.74120

beta = 107.05

c = 6.52490

a/b = 3.25529

Z = 4

i/cor = 7.54

c/b = 1.74407

NIST M&A collection code: N 2978 8216

Temperature factor: [B=O,Ti]

Deleted and rejected by: Deleted: calculated density look very unusual for the given system, SK 2/02.

Data collection flag: Ambient.

T.P. Feist & P.K. Davies, J. Solid State Chem., volume 101, page 275-2 (1992)
Calculated from NIST using POWD-12++

Radiation : CuKα1

Filter : Not specified

Lambda : 1.54060

d-sp : Calculated spacings

SS/FOM : F30=1000(0.000034)

2th	i	h	k	l	2th	i	h	k	l
7.587	999	1	0	0	66.022	1	-1	2	3
13.991	7	-1	0	1	66.418	15	2	0	4
14.186	57	0	0	1	66.418	15	-5	1	4
15.207	38	2	0	0	66.807	1	-3	2	3
17.512	6	-2	0	1	67.125	2	7	1	1
17.979	23	1	0	1	67.270	11	0	2	3
22.895	22	3	0	0	67.270	11	4	1	3
23.152	26	-3	0	1	68.117	9	-6	2	1
23.748	8	2	0	1	68.706	4	6	1	2
24.979	288	1	1	0	68.706	4	5	0	3
27.324	7	-1	0	2	68.258	3	8	1	0
27.783	4	0	1	1	68.427	3	-7	0	4
28.334	97	2	1	0	69.580	4	1	2	3
28.596	52	0	0	2	69.774	3	-9	0	1
29.673	11	-2	1	1	69.774	3	6	2	0
29.799	36	-4	0	1	69.966	3	-6	1	4
29.959	26	1	1	1	69.966	3	-9	0	2
30.461	4	3	0	1	70.202	3	-6	2	2
30.690	10	-4	0	0	71.206	1	4	2	2
31.050	3	-3	0	2	71.642	4	2	1	4
31.777	2	1	0	2	71.642	4	7	0	2
32.235	12	3	1	0	71.813	3	-5	2	3
33.645	11	1	1	1	71.813	3	-8	1	3
35.451	3	-4	0	2	72.638	1	-2	0	5
36.521	31	-1	1	2	72.804	1	2	2	3
37.006	2	-5	0	1	73.064	1	3	0	0
37.199	8	-2	1	2	73.064	1	-4	0	5
37.512	1	0	1	2	73.848	3	5	1	3
37.710	6	4	0	1	73.848	3	-1	0	5
38.405	7	-4	1	1	74.027	2	-9	0	1
38.633	4	3	0	0	74.425	7	-7	2	1
38.998	1	3	1	1	74.817	2	-9	1	1
39.181	1	4	1	0	75.064	4	6	2	1
39.472	1	-3	1	2	75.064	4	-8	1	2
40.065	19	1	1	2	75.651	1	8	1	1
40.976	1	-5	0	2	75.894	3	-7	2	2
41.796	2	-1	0	3	75.894	3	-5	2	3
42.120	1	3	0	2	76.255	2	6	0	4
42.863	1	-3	0	3	76.255	2	0	0	5
43.128	1	-4	1	2	76.495	1	3	1	4
43.486	28	0	0	3	76.589	2	7	2	0
43.953	4	2	1	2	76.811	7	1	3	0
44.456	54	-5	1	1	77.043	3	5	2	2
44.613	43	-6	0	1	77.210	4	3	2	3
45.063	1	4	1	1	77.366	2	4	0	4
45.351	1	5	0	1	77.366	2	-3	1	5
45.537	1	-4	0	3	77.611	1	-2	2	4
46.525	8	1	0	3	77.611	1	-2	1	5
46.775	2	6	0	0	77.929	4	-6	0	5
47.323	3	-6	0	2	77.929	4	-3	2	4
47.917	7	-5	1	2	78.102	2	9	1	0
48.635	39	0	2	0	78.102	2	-4	1	5
48.835	49	-1	1	1	78.352	4	-1	2	4
49.300	11	1	2	0	78.352	4	2	3	0
49.427	6	-5	0	3	78.797	1	-10	0	2
49.994	1	-3	1	3	78.832	2	-1	1	3
50.152	1	0	1	3	79.024	2	-9	1	3
50.726	3	2	0	3	79.024	2	-10	0	1
50.923	3	-1	2	1	79.271	5	-1	2	-1
50.923	3	0	2	1	79.575	3	1	0	5
51.105	18	-6	1	1	80.042	1	-5	1	5
51.256	11	2	2	0	80.042	1	0	2	4
51.832	11	5	1	1	80.532	1	5	0	2
52.000	7	-4	1	3	80.870	3	-7	2	3
52.364	3	1	2	1	80.870	3	3	3	0
52.581	14	-7	0	1	81.190	2	6	1	3
52.897	27	1	1	3	81.190	2	0	1	5
53.124	15	6	1	0	81.560	1	-9	0	4
53.353	5	6	0	1	81.550	1	-8	2	1
54.347	6	-6	0	3	81.719	1	-7	0	5
54.527	7	-3	2	0	82.080	1	-10	0	3
54.818	1	4	1	2	82.279	1	7	1	1
54.818	1	2	2	1	82.279	1	4	1	4
55.175	3	7	0	0	82.452	3	-8	2	2
55.554	8	-5	1	3	82.452	3	4	2	3
55.711	5	5	0	2	82.800	3	-1	5	2
55.908	6	3	0	3	82.800	3	10	0	0
56.319	1	-2	0	4	83.209	1	-2	3	2
56.533	24	-3	0	4	83.400	1	0	3	2
56.753	24	2	1	3	83.756	2	-10	1	2
57.168	2	-2	2	2	83.756	2	6	2	2
57.168	2	-1	0	4	83.963	2	-10	1	1
57.383	10	0	2	2	83.963	2	-4	3	1
58.087	7	-4	2	1					
58.311	9	-4	0	4					
58.476	8	-7	1	1					
58.476	8	3	2	1					
58.614	4	4	2	0					
58.830	2	-3	2	2					
59.196	3	5	1	1					
59.196	3	1	2	2					
60.145	7	-6	1	3					
60.145	7	-7	0	3					
60.809	1	7	1	0					
60.903	1	-5	0	4					
61.407	4	5	1	2					
61.611	5	3	1	3					
61.611	5	-4	2	2					
61.738	3	7	0	1					
61.933	5	-8	0	2					
61.933	5	4	0	3					
62.036	7	-2	1	4					
62.256	3	2	2	2					
62.256	3	1	0	4					
62.349	1	3	1	4					
62.650	1	-5	2	1					
62.816	4	-1	1	4					
63.129	3	4	2	1					
63.390	3	6	0	2					
63.863	2	-4	1	4					
63.863	2	8	0	0					
64.730	4	0	1	4					
64.730	4	-6	0	4					
65.605	1	-7	1	3					
65.867	1	-2	2	3					

Pattern : 00-042-0423		Radiation = 1.540598		Quality : High	
CaTiO ₃		2th		2th	
Calcium Titanium Oxide		i		i	
Perovskite, syn		h		h	
		k		k	
		l		l	
		2th		2th	
		i		i	
		h		h	
		k		k	
		l		l	
		2th		2th	
		i		i	
		h		h	
		k		k	
		l		l	
		2th		2th	
		i		i	
		h		h	
		k		k	
		l		l	
		2th		2th	
		i		i	
		h		h	
		k		k	
		l		l	
		2th		2th	
		i		i	
		h		h	
		k		k	
		l		l	
		2th		2th	
		i		i	
		h		h	
		k		k	
		l		l	
		2th		2th	
		i		i	
		h		h	
		k		k	
		l		l	
		2th		2th	
		i		i	
		h		h	
		k		k	
		l		l	
		2th		2th	
		i		i	
		h		h	
		k		k	
		l		l	
		2th		2th	
		i		i	
		h		h	
		k		k	
		l		l	
		2th		2th	
		i		i	
		h		h	
		k		k	
		l		l	
		2th		2th	
		i		i	
		h		h	
		k		k	
		l		l	
		2th		2th	
		i		i	
		h		h	
		k		k	
		l		l	
		2th		2th	
		i		i	
		h		h	
		k		k	
		l		l	
		2th		2th	
		i		i	
		h		h	
		k		k	
		l		l	
		2th		2th	
		i		i	
		h		h	
		k		k	
		l		l	
		2th		2th	
		i		i	
		h		h	
		k		k	
		l		l	
		2th		2th	
		i		i	
		h		h	
		k		k	
		l		l	
		2th		2th	
		i		i	
		h		h	
		k		k	
		l		l	
		2th		2th	
		i		i	
		h		h	
		k		k	
		l		l	
		2th		2th	
		i		i	
		h		h	
		k		k	
		l		l	
		2th		2th	
		i		i	
		h		h	
		k		k	
		l		l	
		2th		2th	
		i		i	
		h		h	
		k		k	
		l		l	
		2th		2th	
		i		i	
		h		h	
		k		k	
		l		l	
		2th		2th	
		i		i	
		h		h	
		k		k	
		l		l	
		2th		2th	
		i		i	
		h		h	
		k		k	
		l		l	
		2th		2th	
		i		i	
		h		h	
		k		k	
		l		l	
		2th		2th	
		i		i	
		h		h	
		k		k	
		l		l	
		2th		2th	
		i		i	
		h		h	
		k		k	
		l		l	
		2th		2th	
		i		i	
		h		h	
		k		k	
		l		l	
		2th		2th	
		i		i	
		h		h	
		k		k	
		l		l	
		2th		2th	
		i		i	
		h		h	
		k		k	
		l		l	
		2th		2th	
		i		i	
		h		h	
		k		k	
		l		l	
		2th		2th	
		i		i	
		h		h	
		k		k	
		l		l	
		2th		2th	
		i		i	
		h		h	
		k		k	
		l		l	
		2th		2th	
		i		i	
		h		h	
		k		k	
		l		l	
		2th		2th	
		i		i	
		h		h	
		k		k	
		l		l	
		2th		2th	
		i		i	
		h		h	
		k		k	
		l		l	
		2th		2th	
		i		i	
		h		h	
		k		k	
		l		l	
		2th		2th	
		i		i	
		h		h	
		k		k	
		l		l	
		2th		2th	
		i		i	
		h		h	
		k		k	
		l		l	
		2th		2th	
		i		i	
		h		h	
		k		k	
		l		l	
		2th		2th	
		i		i	
		h		h	
		k		k	
		l		l	
		2th		2th	
		i		i	
		h		h	
		k		k	
		l		l	
		2th		2th	
		i		i	
		h		h	
		k		k	
		l		l	
		2th		2th	
		i		i	
		h		h	
		k		k	
		l		l	
		2th		2th	
		i		i	
		h		h	
		k		k	
		l		l	
		2th		2th	
		i		i	
		h		h	
		k		k	
		l		l	
		2th		2th	
		i		i	
		h		h	
		k		k	
		l		l	
		2th		2th	
		i		i	
		h		h	
		k		k	
		l		l	
		2th		2th	
		i		i	
		h		h	
		k		k	
		l		l	
		2th		2th	
		i		i	
		h		h	
		k		k	
		l		l	
		2th		2th	
		i		i	
		h		h	
		k		k	
		l		l	
		2th		2th	
		i		i	
		h		h	
		k		k	
		l		l	
		2th		2th	
		i		i	
		h		h	
		k		k	
		l		l	
		2th		2th	
		i		i	
		h		h	
		k		k	
		l		l	
		2th		2th	
		i		i	
		h		h	
		k		k	
		l		l	
		2th		2th	
		i		i	
		h		h	
		k		k	
		l		l	
		2th		2th	
		i		i	
		h		h	
		k		k	
		l		l	
		2th		2th	
		i		i	
		h		h	
		k		k	
		l		l	
		2th		2th	
		i		i	
		h		h	
		k		k	
		l		l	
		2th		2th	
		i		i	
		h		h	
		k		k	
		l		l	
		2th		2th	
		i		i	
		h		h	
		k		k	
		l		l	
		2th		2th	
		i		i	
		h		h	
		k		k	
		l		l	
		2th		2th	
		i		i	
		h		h	
		k		k	
		l		l	
		2th		2th	
		i		i	
		h		h	
		k		k	
		l		l	
		2th		2th	
		i		i	
		h		h	
		k		k	
		l		l	
		2th		2th	
		i		i	
		h		h	
		k		k	
		l		l	
		2th		2th	
		i		i	
		h		h	
		k		k	
		l		l	
		2th		2th	
		i		i	
		h		h	
		k		k	
		l		l	
		2th		2th	
		i		i	
		h		h	
		k		k	
		l		l	
		2th		2th	
		i		i	
		h		h	
		k		k	
		l		l	
		2th		2th	
		i		i	
		h		h	
		k		k	
		l		l	
		2th		2th	
		i		i	
		h		h	
		k		k	
		l		l	
		2th		2th	
		i		i	
		h		h	
		k		k	
		l		l	
		2th		2th	
		i		i	
		h		h	
		k		k	
		l		l	
		2th		2th	
		i		i	
		h		h	
		k		k	
		l		l	
		2th		2th	
		i		i	
		h		h	
		k		k	
		l		l	
		2th		2th	
		i		i	
		h		h	
		k		k	
		l		l	
		2th		2th	
		i		i	
		h		h	
		k		k	
		l		l	
		2th		2th	
		i		i	
		h		h	
		k		k	
		l		l	
		2th		2th	
		i		i	
		h		h	
		k		k	
		l		l	
		2th		2th	
		i		i	
		h		h	

Appendix B

Fe-doping concentration

The concentration of Fe doped 10% by weight for BTO and Fe doped 2% by weight for CCTO were choosed in this thesis. The process of calculation as shown in equation 1. From WDX experiment shown that Fe concentration of BTO is 7% (data shown in Subsection 5.1.3) and EDX experiment show that Fe concentration of CCTO about 2.5% (data shown in Subsection 5.3.2) by weight instead of 10% and 2% by weight, respectively.

$$\left(\frac{\frac{gFe}{MW_{Fe}}}{\frac{g(Ba/Ca)}{MW_{(Ba/Ca)}}} \right) \left(\frac{MW_{Fe}}{MW_{(BTO/CCTO)}} \right) \times 100 = \dots\dots\% \quad (1)$$

where gFe is weight of Fe, MW_{Fe} is molecular weight of Fe, $g(Ba/Ca)$ is weight of Ba for Fe-doped BTO or weight of Ca for Fe-doped CCTO, $MW_{Ba/Ca}$ is molecular weight of Ba for BTO or Ca for Fe-doped CCTO and $MW_{(BTO/CCTO)}$ is molecular weight of BTO or CCTO, respectively.

Appendix C

Definition

Gray (Gy) is the SI unit of energy for the absorbed dose of radiation.

Absorbed dose is defined as the deposited energy from incident radiation per unit mass of target material, such as air or body tissue.

One gray is the absorption of one joule of radiation energy by one kilogram of matter.

The curie temperature (T_c) is the critical temperature which a previously ferromagnetic material becomes paramagnetic.

Appendix D

Conference presentations

International Presentations:

Kongwut, O. , Kornduangkao, A. , Jangsawang, N. and Hodak, S.K. Influence of gamma irradiation on refractive index of Fe-doped barium titanate thin films. Poster presentation at The Fifth Mathematics and Physical Sciences Graduate Congress, Faculty of Science, Chulalongkorn University, Bangkok (7-9 December 2009)

O. Kongwut, A. Kornduangkao, N. Jangsawang and S.K. Hodak, Influence of gamma irradiation on refractive index of Fe-doped barium titanate thin films. Oral presentation at TACT 2009 International Thin Films Conference, National Taipei University of Technology, Taipei, Taiwan (14-16 December 2009)

Local Presentation:

O. Kongwut, W. Dharmavanij, A. Kornduangkao and S. K. Hodak. Effects of gamma ray irradiation on optical properties of BaTiO_3 thin films prepared by a sol-gel methode. Oral presentation at The Science forum 2009, Faculty of Science, Chulalongkorn University, Bangkok (12-13 March 2009)

O. Kongwut, W. Dharmavanij, A. Kornduangkao and S.K. Hodak. Effects of gamma ray irradiation on optical properties of BaTiO_3 thin films prepared

by a sol-gel method. Poster presentation at Siam Physics Congress 2009, Cha am beach, Phetchaburi (19-21 March 2009)

O. Kongwut, N. Jangsawang, A. Kornduangkaeo and S.K. Hodak. Optical properties of Fe-doped calcium copper titanate thin films under gamma irradiation. Poster presentation at The 16th national graduate Research Conference, Maejo University, Sansai, Chiang Mai (11-12 March 2010)

Satreerat K. Hodak, **O. Kongwut**, N. Jangsawang and A. Kornduangkaeo. Optical properties of Fe-doped barium titanate thin films under gamma irradiation. Oral presentation at The Science forum 2009, Faculty of Science, Chulalongkorn University, Bangkok (11-12 March 2010)

O. Kongwut, N. Jangsawang, A. Kornduangkaeo and S.K. Hodak. Optical properties of Fe-doped calcium copper titanate thin films under gamma irradiation. Oral presentation at Siam Physics Congress 2010, River Kwai Village Hotel, Kanchanaburi (25-27 March 2010)

Appendix E

Publications

O. Kongwut, A. Kornduangkaeo, N. Jangsawang and S.K. Hodak, Influence of gamma irradiation on refractive index of Fe-doped barium titanate thin films. (Thin Solid Films).

O. Kongwut, A. Kornduangkaeo, N. Jangsawang and S.K. Hodak, Optical properties of Fe-doped calcium copper titanate thin films under gamma irradiation. (Proceeding).



Influence of gamma irradiation on the refractive index of Fe-doped barium titanate thin films

O. Kongwut^a, A. Kornduangkeaw^b, N. Jangsawang^b, Satreerat K. Hodak^{a,c,*}

^a Department of Physics, Faculty of Science, Chulalongkorn University, Bangkok 10330, Thailand

^b Thailand Institute of Nuclear Technology (TINT), Bangkok 10900, Thailand

^c Center of Innovative Nanotechnology, Chulalongkorn University, Bangkok 10330, Thailand

ARTICLE INFO

Available online 10 May 2010

Keywords:
Gamma irradiation
Fe-doped BaTiO₃
Sol–gel method
Refractive index

ABSTRACT

Polycrystalline Fe-doped barium titanate (Fe-doped BaTiO₃) thin films were grown by thermal decomposition of the precursors deposited from a sol–gel system onto quartz substrates. The changes in the transmittance spectra induced by gamma irradiation on the Fe-doped BaTiO₃ thin films were quantified. The values for the optical energy band gap were in the range of 3.42–3.95 eV depending on the annealing time. The refractive index of the film, as measured in the 350–750 nm wavelength range was in the 2.17–1.88 range for the as prepared film, and this increased to 2.34–1.95 after gamma irradiation at 15 kGy. The extinction coefficient of the film was in the order of 10^{−2} and increased after gamma irradiation. We obtained tuneable complex refractive index of the films by exposure to various gamma rays doses.

© 2010 Elsevier B.V. All rights reserved.

1. Introduction

Recently, the effects of the inclusion of different transition metals on the structural, optical, electrical and magnetic properties of perovskite (ABO₃) thin films have been investigated. Various types of dopants and cations of different sizes can be accommodated in the ABO₃ sites [1–4]. Barium titanate (BaTiO₃) is a ferroelectric material with a perovskite structure (Ba²⁺ as A and Ti⁴⁺ as B) that has gained much interest due to its many potential applications, such as high dielectric constant capacitors, dynamic random access memories, and piezoelectric and optical wave guide devices [5–7]. In addition, doping Fe ions into the BaTiO₃ lattice leads to the acquisition of both ferromagnetic and ferroelectric properties [8]. The ferromagnetism of Fe-doped BaTiO₃ ceramics was reported to be dependent upon the annealing atmosphere and Fe-doping concentration, with the substitution by Fe³⁺ occurring in Ti sites being confirmed by Mossbauer measurements [9,10]. Herner et al. showed that doping barium strontium titanate (BaSrTiO₃) with Fe could reduce the loss tangent [11], by means of improving the dielectric properties compared to pure BaSrTiO₃. Another way to change the fundamental properties of these materials is by exposure to high energy electromagnetic radiation or high energy particles, such as X-rays, gamma rays, electron or neutron bombardment. The retained polarization, dielectric constant and coercive field of lead titanate films decreased upon increasing gamma irradiation doses, but the material was less sensitive to neutron irradiation [12]. Recently, Arshak et al. observed that the energy gap of a bismuth germanate film decreased

from 1.95 eV to 1.76 eV after exposure to gamma irradiation with a 0.228 mGy of gamma irradiation [13]. Fasasi et al. have reported the use of high dose gamma irradiation to study the thermoluminescence glow curve characteristic of BaTiO₃ ceramics and the dose dependence on the glow curve [14]. These radiation imparted changes in BaTiO₃ are extremely useful for the effective design of modern radiation dosimeters.

In this work, the effect of gamma ray irradiation on the optical properties of Fe-doped and undoped BaTiO₃ thin films was investigated. The changes in transmittance spectra induced by gamma irradiation, and the corresponding changes in the film refractive index and extinction coefficient, were measured as a function of the gamma irradiation dose.

2. Experimental details

BaTiO₃ and Fe-doped BaTiO₃ thin films were deposited on quartz substrates by a sol–gel method. The Fe-doping process was done by dissolving iron (II) sulphate (FeSO₄) in a mixture of barium acetate (Ba(CH₃COO)₂) and acetic acid. Then, pure titanium n-butoxide and methanol were added to the solution. The precursor solution was dropped onto the clean quartz substrate with a spinning speed of 1500 rpm to provide the first layer of the film. The film was preheated at 120 °C for 20 min before annealing in an atmosphere of air at 800 °C for 60 min in order to form the crystalline structure. This process was repeated until the desired thickness was obtained. Different film thicknesses can be obtained by varying the number of deposition cycles. A ⁶⁰Co gamma radiation source with an activity of 10 kCi (Gammacell 220 Excell) was used to irradiate the BaTiO₃ and Fe-doped BaTiO₃ thin films. The radiation doses were varied via the exposure time up to 15 kGy at a rate of 10 kGy/h. The optical transmittance

* Corresponding author. Department of Physics, Faculty of Science, Chulalongkorn University, Bangkok, 10330, Thailand.
E-mail address: satreerat@chula.ac.th (S.K. Hodak).



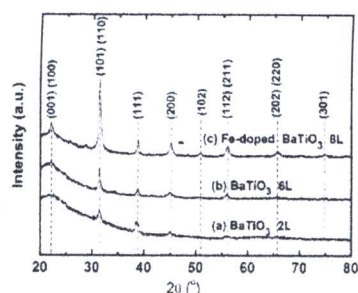


Fig. 1. X-ray diffraction patterns of (a) BaTiO_3 film with 2 layers, (b) BaTiO_3 film with 6 layers, (c) Fe-doped BaTiO_3 film with 8 layers.

spectra of the films were measured using a Perkin-Elmer Lambda 750 UV–Vis–NIR spectrophotometer. The refractive index and the extinction coefficient of the films before and after gamma irradiation as a function of the gamma dose were extracted from the transmittance spectra using the envelope method [15]. The band gap was also calculated from the transmittance spectra using the Tauc relation [16]. The compositions of the films were obtained using a wavelength dispersive X-ray spectrometer (WDX) equipped with an electron probe microscopic spectrometer (EPMS; JEOL model JXA-8100). The oxidation state of Fe in the Fe-doped BaTiO_3 films was examined by X-ray absorption spectroscopy near the edge structure (XANES) using a synchrotron source. The X-ray diffraction (XRD; Bruker model D8-Discover) patterns of BaTiO_3 and Fe-doped BaTiO_3 films were recorded to determine their crystal structures. The surface morphology of the films was observed using a Veeco Nanoscope IV atomic force microscopy (AFM).

3. Results and discussion

3.1. Structural properties

The substitution site for the dopant cation depends more strongly on its concentration and on the Ba/Ti molar ratio than on its size [17]. The ionic radius of Fe^{3+} (0.64 Å) is comparable with the ionic radius of Ti^{4+} (0.68 Å) but is significantly different from that of Ba^{2+} (1.34 Å) [4]. However, the WDX shows signals that are consistent with $\text{Ba}_{0.9}\text{Fe}_{0.2}\text{TiO}_3$ with the Fe doping occurring by substitution of Ba sites in BaTiO_3 yielding a Ba/Ti ratio slightly smaller than 1. The oxidation state determined from the energy of the X-ray absorption edge (7130.5 eV) corresponds to Fe^{3+} . In our case the Fe^{3+} dopant acts

as a donor when it substitutes the Ba^{2+} site. A similar result for this substitution was found in the work of Battisha et al. [1].

The crystallinity of the films was investigated using X-ray diffraction. Fig. 1 shows the XRD patterns of undoped BaTiO_3 with two and six layers as well as that for Fe-doped BaTiO_3 films with eight layers, derived from a sol–gel method. We denoted each film by the material formula followed by the number of layers (L). The tetragonal phase of BaTiO_3 was identified in our films and it is indicated in Fig. 1 by the peaks with the indices of its crystallographic planes. The diffraction peaks are sharper and more intense as the films grow thicker through the deposition of more layers. The peak positions slightly shifted to higher diffraction angles after doping Fe in the film indicating that the lattice constants slightly decreased. This could be attributed to the substitution of ions with smaller size (Fe^{3+}) to ions with bigger size (Ba^{2+}). These results are consistent with the work of other groups [4,18].

The surface morphology of BaTiO_3 and Fe-doped BaTiO_3 films was investigated by atomic force microscopy (AFM), where the estimated average grain size of the $\text{Ba}_{0.9}\text{Fe}_{0.2}\text{TiO}_3$ 8 L film at 40 nm is smaller than the 54 nm grain size for the 6 L film as seen in Fig. 2. Devan et al. observed similar results with a decrease in grain size with doping concentrations [18]. Indeed, many research groups have reported that increasing the dopant concentration could reduce the grain size due to competition between different phase structures in the materials [2,4,19,20].

3.2. Optical properties

Fig. 3 shows the optical transmission spectra in the 300–1200 nm wavelength range of the undoped BaTiO_3 and Fe-doped BaTiO_3 films of comparable thickness (ca. 220 nm) before and after gamma irradiation at 15 kGy. The oscillation in the transmission curve is due to interference between light reflecting from the film surface and from the film–substrate interface. The depth of modulation indicates good homogeneity of the films across the light beam (ca. 1 cm in diameter). The transmittance of both undoped and Fe-doped films was reduced after the irradiation, and a brownish tint could be seen by the naked eye in the irradiated films. However, our results revealed that gamma irradiation causes a more marked change on the transmittance of the Fe-doped BaTiO_3 film than to the undoped film. For comparison, following gamma irradiation at 15 kGy, the transmittance decreased by ~4% in the undoped BaTiO_3 film but by ~11% for the $\text{Ba}_{0.9}\text{Fe}_{0.2}\text{TiO}_3$ film. It seems that the trapping process in the films after irradiation occurs more readily in the doped films, presumably because they have more defects than in undoped films. There are two types of defects in barium titanate: the type that preserves the stoichiometry (Schottky) and the type that changes the stoichiometry that occurs at the dopant substituted cells. Oxygen vacancy defects are commonly found in

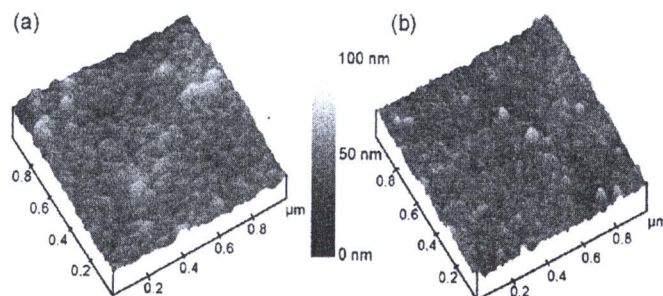


Fig. 2. Atomic force microscopy (images $1.0 \times 1.0 \mu\text{m}^2$) of the films comprised of (a) BaTiO_3 with 6 layers (b) Fe-doped BaTiO_3 with 8 layers.

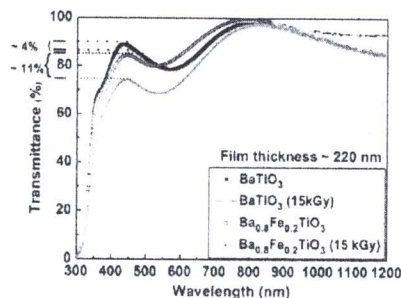
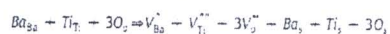


Fig. 3. The transmission spectra of BaTiO_3 and $\text{Ba}_{0.8}\text{Fe}_{0.2}\text{TiO}_3$ thin films before and after gamma irradiation at a dose of 15 kGy.

BaTiO_3 due to an insufficient oxygen supply during the film processing [21]. Intrinsic Schottky defects in BaTiO_3 are believed to form according to the following process: [14],



where Ba_{Ba} , Ti_{T} , O_{O} are occupied Ba, Ti and O sites, respectively, $V_{\text{Ba}}^{\bullet\bullet}$, $V_{\text{T}}^{\bullet\bullet}$ and $3V_{\text{O}}^{\bullet\bullet}$ are vacancies of Ba, Ti and O atoms, respectively, and Ba_s , Ti_s and O_s are the Schottky defects, respectively. Upon irradiation there are a number of phenomena that can give rise to trap sites in BaTiO_3 . For example, a negative ion could be removed and this ion vacancy can subsequently trap an electron which constitutes the so-called F-center [14]. Another pathway is the self-trapping of holes [22]. Fig. 4(a) shows the optical transmission spectra of Fe-doped BaTiO_3 films with four and six layers (denoted by $\text{Ba}_{0.8}\text{Fe}_{0.2}\text{TiO}_3$ 4L and $\text{Ba}_{0.8}\text{Fe}_{0.2}\text{TiO}_3$ 6L, respectively) in the 300–1200 nm wavelength range and Fig. 4(b) shows the same trend for the Fe-doped BaTiO_3 film with eight layers (denoted by $\text{Ba}_{0.8}\text{Fe}_{0.2}\text{TiO}_3$ 8L). As expected, the thicker film shows deeper oscillations in the transmission spectrum than the thinner film. The transmittance also decreased with the increasing gamma radiation doses. The doses used in this study were 1, 5, 10 and 15 kGy, respectively. We observed that the transmittance of the films did not change any further for gamma radiation doses higher than ca. 10 kGy. The absorption edge shifted to a lower energy as the films got thicker (Fig. 4(a)), because the films with a larger number of layers accumulated longer heating times (800 °C for 60 min for each layer) causing the growth of bigger grains. However, there was little variation in the absorption edge between the $\text{Ba}_{0.8}\text{Fe}_{0.2}\text{TiO}_3$ 4L film annealed for 4 h and $\text{Ba}_{0.8}\text{Fe}_{0.2}\text{TiO}_3$ 8L film annealed for 8 h. The film thickness of $\text{Ba}_{0.8}\text{Fe}_{0.2}\text{TiO}_3$ ranging from four to eight layers was calculated via the envelope method derived by Swanepoel [23] and was approximately 220 nm (4L), 375 nm (6L) and 520 nm (8L). From the transmittance spectra, the energy for the direct gap could be calculated by using the Eq. (1)

$$(\alpha h\nu)^2 = B(h\nu - E_g) \quad (1)$$

Where α is the absorption coefficient calculated by $\alpha = \frac{1}{d} \ln \frac{I_0}{I}$, $h\nu$ is the photon energy, E_g is the energy gap and B is a constant [16]. Fig. 5 shows a plot between $(\alpha h\nu)^2$ versus $h\nu$ (eV) of the Fe-doped BaTiO_3 thin films with 4, 6 and 8 layers of thin films. The resulting energy band gaps were 3.42 eV, 3.69 eV and 3.95 eV for $\text{Ba}_{0.8}\text{Fe}_{0.2}\text{TiO}_3$ with 8, 6 and 4 layers, respectively. For comparison, the energy band gap value of pure BaTiO_3 powder, BaTiO_3 single crystal, and BaTiO_3 thin films are 3.92 eV [24], 3.6 eV [25] and 3.72–3.77 eV [26], respectively. The particle size in these films increases as the annealing cycle increases

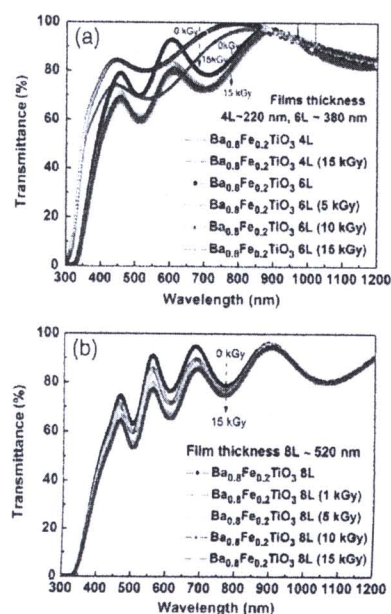


Fig. 4. The transmission spectra of (a) $\text{Ba}_{0.8}\text{Fe}_{0.2}\text{TiO}_3$ films with 4 and 6 layers and (b) $\text{Ba}_{0.8}\text{Fe}_{0.2}\text{TiO}_3$ films with 8 layers, after exposure to different gamma radiation doses.

[27]. The corresponding reduction in band gap energy with increasing particle size can be explained by quantum confinement [28,29]. The refractive index can be obtained using an envelope method:

$$n(\lambda) = \left[N - \left(N^2 - n_s^2 \right)^{1/2} \right]^{1/2} \quad (2)$$

where $N = \left(\frac{n_s^2 - 1}{2} \right) - 2n_s^2 \left(\frac{T_{\text{max}} - T_{\text{min}}}{T_{\text{max}} + T_{\text{min}}} \right)$, n_s is the refractive index of the substrate, T_{max} and T_{min} are the maximum and minimum transmittances. The extinction coefficient can be obtained from

$$k = \frac{\lambda \alpha}{4\pi} \quad (3)$$

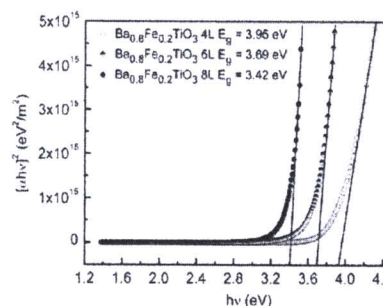


Fig. 5. Plot between $(\alpha h\nu)^2$ versus $h\nu$ (eV) of $\text{Ba}_{0.8}\text{Fe}_{0.2}\text{TiO}_3$ thin films with 4, 6 and 8 layers.

where λ is the wavelength, α is the absorption coefficient ($\alpha = \frac{1}{d} \ln \frac{(n-1)(n_2+n)}{(n+1)(n_2-n)} \frac{1 - (T_{\text{max}}/T_{\text{min}})^2}{1 - (T_{\text{max}}/T_{\text{min}})^2}$) and d is the film thickness.

Analysis of the variation of the dispersion curves of $\text{Ba}_{0.8}\text{Fe}_{0.2}\text{TiO}_3$ films after different (0–15 kGy) gamma irradiation doses reveal that the refractive index and the extinction coefficient increase with the wavelength rising more rapidly toward short wavelengths and following a typical dispersion curve shape (Fig. 6). When measured in the 350–750 nm wavelength range, the refractive index for the $\text{Ba}_{0.8}\text{Fe}_{0.2}\text{TiO}_3$ 4 L increased from the 2.17–1.88 range to the 2.34–1.95 range upon the gamma irradiation at a dose of 15 kGy, with a corresponding

increase in the extinction coefficient (Fig. 6(a) and (b)). The value of the extinction coefficient for this film prior to gamma irradiation was in the order of 10^{-2} and this increased after the irradiation with higher doses, indicating that higher optical losses result directly from the irradiation. With thicker films, the refractive index is also increased due to the increased film density and better crystallinity. The extinction coefficient follows an approximately linear function of the wavelength. The dispersion curves near the electronic band transition were significantly altered by the gamma irradiation. One of the main results of these experiments is that the complex refractive index of the films can be tuned by exposure to various gamma rays doses. These observed phenomena could be useful for the development of gamma irradiation dosimeters based on simple optical detection properties.

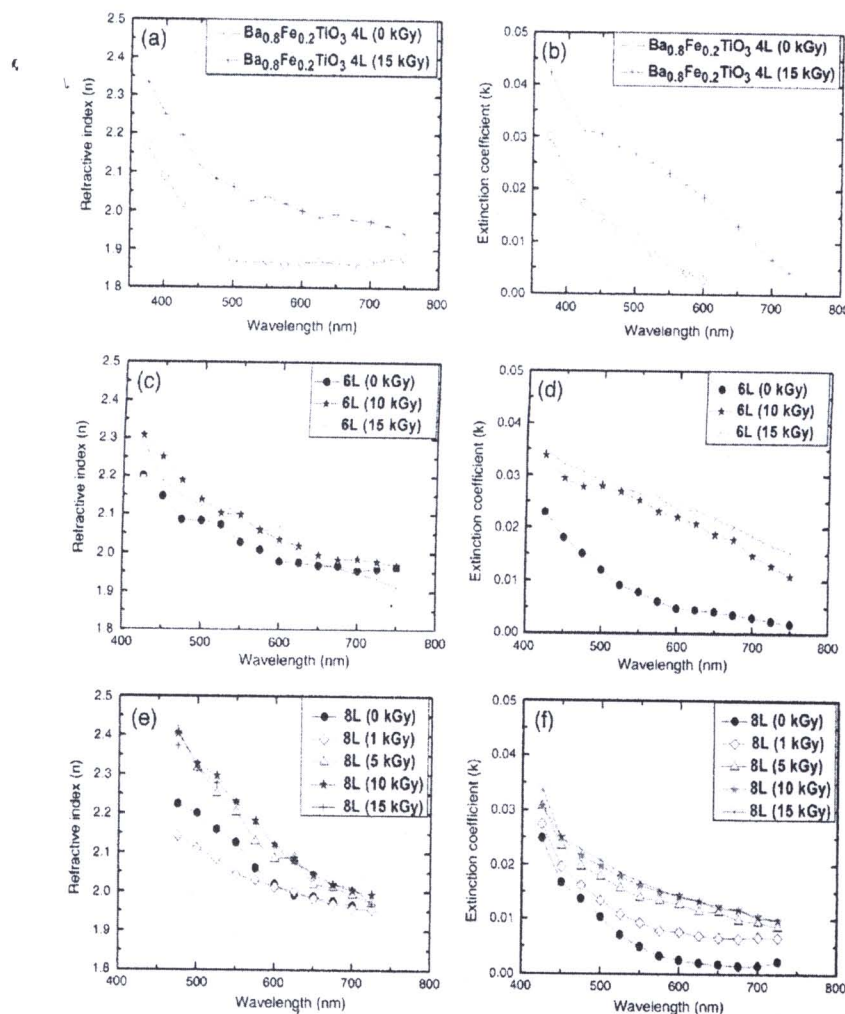


Fig. 6. (a,c,e) The refractive index of $\text{Ba}_{0.8}\text{Fe}_{0.2}\text{TiO}_3$ thin films with 4, 6 and 8 layers, respectively and (b,d,f) the extinction coefficient of $\text{Ba}_{0.8}\text{Fe}_{0.2}\text{TiO}_3$ thin films with 4, 6 and 8 layers, respectively.

4. Conclusions

Gamma irradiation effects were found to be more pronounced for the iron doped films ($\text{Ba}_{0.8}\text{Fe}_0.2\text{TiO}_3$) than for the undoped BaTiO_3 . The transmittance of the films in the UV–visible range decreased after gamma irradiation with doses in the 1–15 kGy range. The refractive index and the extinction coefficient of the films were increased by exposure to higher gamma ray doses. These changes are due to the formation of color centers and the concomitant change in the complex refractive index for the irradiated the $\text{Ba}_{0.8}\text{Fe}_0.2\text{TiO}_3$ films.

Acknowledgments

This work was supported by The Thailand Research Fund (TRF), the Thailand Toray Science Foundation (TTSF), National Research Council of Thailand (NRCT) and a Graduate Thesis Grant. Also, this work was supported by Research Funds from the Faculty of Science, Chulalongkorn University (A1B1), the Thai Government Stimulus Package 2 (TKK2555) under the Project for Establishment of Comprehensive Center for Innovative Food, Health Products and Agriculture, and Chulalongkorn University Centenary Academic Development Project. The authors would like to thank the Synchrotron Light Research Institute at Suranaree University of Technology.

References

- [1] I.K. Battista, A.B.A. Hamad, R.M. Mahani, *Phys. B* 404 (2009) 2274.
- [2] E. Brzozowski, M.S. Castro, *J. Mater. Process. Technol.* 168 (2005) 464.

- [3] K. Daoudi, T. Tsuchiya, T. Kumagai, *Appl. Surf. Sci.* 253 (2007) 6527.
- [4] Y. Ye, T.L. Guo, *Ceram. Int.* 35 (2009) 2761.
- [5] S. Xu, H. Huang, H. Fan, H.J.W. Chan, L.M. Zhou, *Solid State Ionics* 179 (2008) 1632.
- [6] F. Zimmermann, M. Voigt, W. Menesklou, E. Ivers-Tiffée, *J. Eur. Ceram. Soc.* 24 (2004) 1729.
- [7] A. Kumar, S.G. Manavalan, *Surf. Coat. Technol.* 198 (2005) 406.
- [8] T.K. Kundu, A. Jana, P. Barik, *Bull. Mater. Sci.* 31 (2008) 501.
- [9] F. Lin, D. Jiang, X. Ma, W. Shi, *Phys. B* 403 (2008) 2525.
- [10] F. Lin, D. Jiang, X. Ma, W. Shi, *J. Magn. Magn. Mater.* 302 (2008) 691.
- [11] S.B. Heinen, F.A. Selim, V.V. Varadan, V.K. Varadan, *Mater. Lett.* 15 (1993) 317.
- [12] J. Gao, L. Zheng, Z. Song, C. Lin, D. Zhu, *Mater. Lett.* 42 (2000) 345.
- [13] K. Arshak, O. Korostynska, J. Harris, D. Morris, A. Arshak, E. Jeter, *Thin Solid Films* 516 (2008) 1493.
- [14] A.Y. Fasasi, F.A. Balogun, M.K. Fasasi, P.O. Ogunleye, C.E. Mokobia, E.P. Inyang, *Sens. Actuators A* 135 (2007) 596.
- [15] M. Caglar, Y. Caglar, S. Iscan, *J. Optoelectron. Adv. Mater.* 8 (2006) 1410.
- [16] J. Tauc, A. Menth, *J. Non-Cryst. Solids* 8–10 (1972) 569.
- [17] M.T. Buscaglia, V. Buscaglia, M. Viviani, P. Nanni, M. Hanuskova, *J. Eur. Ceram. Soc.* 20 (2000) 1997.
- [18] R.S. Devan, Y.R. Ma, B.K. Chougale, *Mater. Chem. Phys.* 115 (2009) 263.
- [19] Y.C. Huang, W.H. Tuan, *Mater. Chem. Phys.* 105 (2007) 320.
- [20] S.Y. Lee, B.S. Chou, H.J. Lu, *Mater. Chem. Phys.* 108 (2008) 55.
- [21] K. Shimoyama, K. Kubo, T. Maeda, K. Yamabe, *Jpn. J. Appl. Phys.* 40 (2001) 463.
- [22] A. Stashans, H. Pinto, *Radiat. Meas.* 33 (2001) 553.
- [23] R.S. Swanepoel, *J. Phys. E Sci. Instrum.* 16 (1983) 1214.
- [24] A. Mansingh, C.V.R. Vasanta, *J. Mater. Sci. Lett.* 7 (1988) 1104.
- [25] A. Onton, V. Marelli, G. Lucovsky, F.L. Galeener (Eds.), *AIP Conf. Proc. No. 31*, AIP, New York, 1976.
- [26] H.X. Zhang, C.H. Kam, Y. Zhou, X.Q. Han, Y.L. Lam, Y.C. Chan, K. Pua, *Mater. Chem. Phys.* 63 (2000) 174.
- [27] X.M. Lu, J.S. Zhu, W.Y. Zhang, G.Q. Ma, Y.N. Wang, *Thin Solid Films* 274 (1996) 165.
- [28] L. Burns, *J. Phys. Chem.* 90 (1986) 2555.
- [29] T. Supasai, S. Dangup, P. Learningarun, N. Boonyapaxum, A. Wisitsaraat, Sattreevat K. Hodek, *Appl. Surf. Sci.* 256 (14) (2010) 4462.

ภายใต้การฉายรังสีแกมมา

OPTICAL PROPERTIES OF FE-DOPED CALCIUM COPPER TITANATE THIN FILMS UNDER GAMMA IRRADIATION

อณิชา คงามณี อาริรัตน์ คอนดองแก้ว นงนช แจงสว่าง และ สตรีรัตน์ ไพบูลย์

Omnilna Kongwut^a, Areearat Kornduangkeaw^a, Nongnuch Jangsawang^a, and S.K. Hodak^b

บทคัดย่อ

[illegible]

Abstract

© 2009 Game magazine, Inc. All rights reserved. Online only.

Figure 1. The effect of the concentration of the *Agrobacterium* suspension on the transformation efficiency of *Agrobacterium* strains. The *Agrobacterium* strains were grown in YEA medium for 24 h at 28 °C. The cell concentration was adjusted to 10⁸ cells/ml. The cells were then mixed with the plant tissue and the transformation efficiency was determined. The results are shown as the mean ± SD of three independent experiments. The transformation efficiency was significantly different from the control (p < 0.05).

Introduction

Calcium copper manganate ($\text{CaCu}_2\text{Mn}_2\text{O}_{10}$, CCMO) is a novel ferroelectric material with high dielectric constant values and it does not show ferroelectric transition in the temperature range of 200K–600K. In the past few decades, many applications such as high dielectric constant capacitors and dynamic RAMs [1]–[4] (2003, Fang and Shen, 2008, and Liu et al., 2007) have been dealt with CCMO due to the unchanged dielectric constant over a wide range of temperature and frequency. There are several methods to modify the film properties such as controlling the growth parameters, changing the growth techniques and doping with various types of dopants. It has been reported that doping Fe in the CCMO films [5, 6] alter the temperature dependence of dielectric constant and the reduction in dielectric constant [7, 8] (2005). It is worthy to investigate another way to change the electrical and optical properties of CCMO after finishing the regular film processing. Exposure materials with high energy electromagnetic radiations or high energy particles such as X-rays, gamma rays, electrons or neutrons are considered as post processing. For example, Arshak et al. observed that the energy gap of bismuth germanate film was reduced from 1.92 eV to 1.76 eV after exposure to gamma irradiation with a 0.028 mGy dose [Arshak et al., 2019].

In this work, the effects of gamma ray radiation on optical properties of Fe-doped calcium copper manganate thin films were investigated. The changes in transmittance spectra induced by gamma radiation, and the corresponding changes in refractive index and extinction coefficient of the films were measured as a function of gamma radiation doses. Studying the effect of gamma radiation is important to design the modern dosimeters.

Experimental Methods

Fe-doped calcium copper manganate thin film was deposited on quartz substrate by a sol-gel spin coating technique. Quartz has been suitable substrates for studying the transmission of the materials being deposited due to its transparency and high temperature melting point. In the precursor processing, iron(III) sulphate (Fe_2SO_4), copper acetate and calcium acetate were firstly dissolved in acetic acid, and then titanium isopropoxide was slowly added. Ethylene glycol and formamide were added into the solution in order to increase solution stability. In this step, the solution viscosity can be also controlled to prevent the film cracking during the baking and annealing. The precursor solution was dropped on the clean quartz substrate with the spinning speed of 1500 rpm. The film was preheated at 120 °C for 20 min before annealing in the atmosphere at 600 °C annealing temperature for 60 min. We investigated the effects of the ^{60}Co (GammaCell 220 Excel) gamma radiation on the changes in optical properties of CCMO and Fe-doped CCMO thin films. In this study, the activity of gamma ray was 10 kCi and the exposure rate was 10 CGy/hr. The films were placed in the centre of the reactor and the doses of gamma radiation were varied up to 5 mGy. The optical transmittance spectra of the films were measured

using PerkinElmer Lambda 1050 UV-Vis-NIR Spectrophotometer. The refractive index and the extinction coefficient of the films before and after gamma radiation as a function of gamma dose were extracted from transmittance spectra using ellipsence method (Calet et al., 2016). The band gap was calculated from the transmittance spectra.

Results and discussion

Fig. 1 shows the optical transmission spectra in the 300–1200 nm wave-length range of Fe-doped $\text{CaCu}_2\text{Ti}_2\text{O}_{10}$ films before and after gamma radiation at 1, 3, and 6 kGy dose respectively. The domain of transmission normality indicates that the films are homogeneous. We have found the reduction in transmittance decreasing to 1.5% and 4.8% after exposure with gamma radiation dose at 1 kGy and 6 kGy, respectively. We observed that the transmittance of the films did not change after the gamma radiation dose 3 kGy. In another word, there was not much change in the transmittance for the film exposed at 1, 3, and 6 kGy. This could be due to the saturation of activity of each centre (chromophore) under irradiation. In general, the absorption of the film could be employed and this, in turn, can subsequently radiate electron, which is separated (Fowler, 1988) for the separation of holes and electrons (Stashans and Pints, 2010). From the transmittance spectra, the energy band gap for direct gap could be calculated by using the Equation (1).

$$(\alpha h\nu)^2 = B(h\nu - E_g)$$
 (1)

where G is the absorption coefficient of the film and $\alpha = \frac{1}{d} \ln \frac{1}{T}$, d is the thickness of the film, E_g is energy band gap and B is a constant. Fig. 2 shows plot between $(\alpha h\nu)^2$ vs $h\nu$ for Fe-doped $\text{CaCu}_2\text{Ti}_2\text{O}_{10}$ thin films. The resulting energy band gaps were 3.67 eV. For comparison, the energy band gap value of $\text{CaCu}_2\text{Ti}_2\text{O}_{10}$ thin films is 3.65 eV (Togiani et al., 2019). The discrepancy will be further investigated. The refractive index can be obtained using envelope method:

$$n(\lambda) = [N + (N^2 - n^2)^2]^{-1/2}$$
 (2)

where $N = (\frac{n^2 - 1}{2}) + 2n_s(\frac{T_{\text{max}} - T_{\text{min}}}{T_{\text{max}} + T_{\text{min}}})$, n_s is the refractive index of the substrate, T_{max} and T_{min} are the maximum and minimum transmittance. The extinction coefficient can be obtained from

$$k = \frac{2\alpha}{4\pi}$$
 (3)

where α is the absorption coefficient, $\alpha = \frac{1}{d} \ln \frac{(n+1)(n+m)[1-(T_{\text{ext}}/T_{\text{int}})^2]}{(n-1)(n-m)[1-(T_{\text{ext}}/T_{\text{int}})^2]}$, and d is the film thickness. The film thickness was simply determined through the equation:

$$d = \frac{\lambda_1 \lambda_2}{2(m\lambda_1)^2 - m(\lambda_2)^2} \quad (4)$$

Where $m(\lambda_1)$ and $m(\lambda_2)$ are refractive indices of two adjacent medium at wavelength λ_1 and λ_2 , respectively. The calculated thickness was 360 nm.

Fig. 3 shows the refractive index and the extinction coefficient of the Fe-doped $\text{CaCu}_3\text{Ti}_2\text{O}_{12}$ film measured in the 350–750 nm wavelength range. The refractive index of the films measured in the 450–700 nm wavelength range increased from 1.76 ± 0.05 range to 1.97 ± 0.03 range for Fe-doped $\text{CaCu}_3\text{Ti}_2\text{O}_{12}$ film under the gamma irradiation with a 2 kGy dose with a corresponding increase in the extinction coefficient as shown in Fig. 4. There was not much change in the refractive index of the films until the dose increased to 2 kGy. The increase in the extinction coefficient with the irradiation dose indicates that high color losses caused by the irradiation. The increase in the extinction coefficient with the irradiation dose indicates that high color losses caused by the irradiation. The value of the extinction coefficient of the films before and after gamma irradiation was still on the order of 10^3 . The shape of refractive index was similar to the result of Raffaele et al. group (Raffaele et al., 2006).

Conclusions

The parameters of Fe-doped $\text{CaCu}_3\text{Ti}_2\text{O}_{12}$ films was reduced after gamma irradiation in the dose range of 1–2 kGy. The refractive index of as a function of wavelength the Fe-doped $\text{CaCu}_3\text{Ti}_2\text{O}_{12}$ films can be change by exposure to gamma rays doses higher than 1 kGy where as the change in extinction coefficient could be observed with exposure only 1 kGy.

Acknowledgement

The work was supported by The Thailand Research Fund (TRF), the Thailand Topical Foundation (TF), National Research Council of Thailand (NRCT) and Graduate Thesis Grant. The authors would like to thank Thai and Institute of Nuclear Technology (INT) for the help in gamma irradiation experiment.

References

- Li, Y.W., Hu, Z.G., Sun, J.L., Meng, X.J. and Chen, J.F.: 2008, Preparation and properties of $\text{CaCu}_3\text{Ti}_2\text{O}_{12}$ thin film grown on LaAlO_3 coated silicon by sol-gel process, *Journal of Crystal Growth* 311, 376.
- Fang, L. and Shen, M.: 2003, Detection and dielectric properties of $\text{CaCu}_3\text{Ti}_2\text{O}_{12}$ thin films on $\text{PbTiO}_3/\text{SiO}_2/\text{Si}$ substrates using pulsed-laser deposition, *Thin Solid Films* 442, 60.
- Li, J., Fan, H., Fang, P. and Jin, L.: 2007, Electric heterogeneity in $\text{CaCu}_3\text{Ti}_2\text{O}_{12}$ ceramics fabricated by sol-gel method, *Solid State Communications* 142, 573.

Quares, R.K., Verma, B.C., Devi, P., Achary, J.J., Tane, B.A. and Sankar, G.A., 2005, Dielectric and magnetic properties of Fe-doped $\text{CaCu}_3\text{Ti}_4\text{O}_{12}$. *Physical Review B* 72:1404.

Arslan, R., Kucuk, O., Haktanir, J., Muris, B., Kucuk, A. and Yeter, E., 2008, Properties of BiO thin films under the influence of gamma radiation. *Thin Solid Films* 516:1493.

Qayyum, M., Qayyum, S. and Javed, S., 2018, Preparation and characterization of ZnO thin films deposited by sol-gel spin coating method. *Journal of Optoelectronics and Advanced Materials* 12:1410.

Fazal, A., Baigun, F.A., Fazal, M.K., Quney, P.O., Moxco, C.E. and Myang, B.P., 2007, Thermoluminescence properties of calcium titanate prepared by solid-state reaction. *Sensors and Actuators A* 137:540.

Shahans, A. and Rino, H., 2001, Analysis of radiation-induced hole localisation in titanates. *Radiation Measurements* 33:553.

Ting, H., Qiang, C., Yueheng, Z., Heng, L., Dongfang, Z., Ha, M. and Guizhen, Y., 2009, Large surface area $\text{Fe-doped CaCu}_3\text{Ti}_4\text{O}_{12}$ thin films. *Applied Physics* 4:491507.

Raffaella, L., Ferrara, G.T., Basso, A., Mignone, L.F., Vona, L., Monella, M.G., Giovanni, B., Vito, R. and Paoletti, F., 2018, Calcium Copper Titanate Thin Film Growth: Tailoring of the Operational Conditions through Nanocrystallization and Substrate Nature Effects. *Journal of Physical Chemistry B* 122:10280.

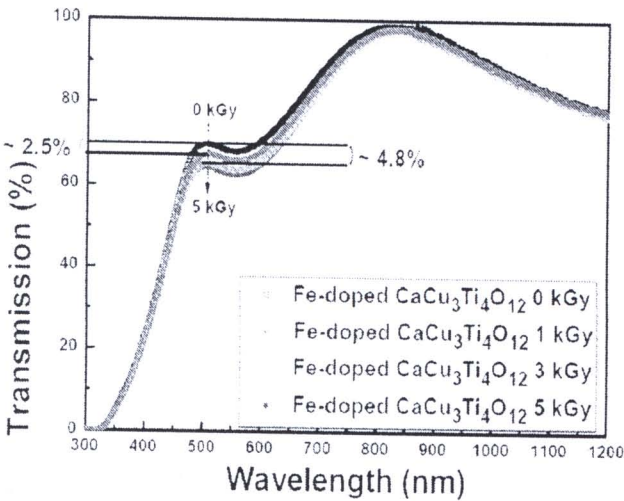


Figure 1. The transmission spectra of Fe-doped $\text{CaCu}_3\text{Ti}_4\text{O}_{12}$ thin films for different gamma radiation dose

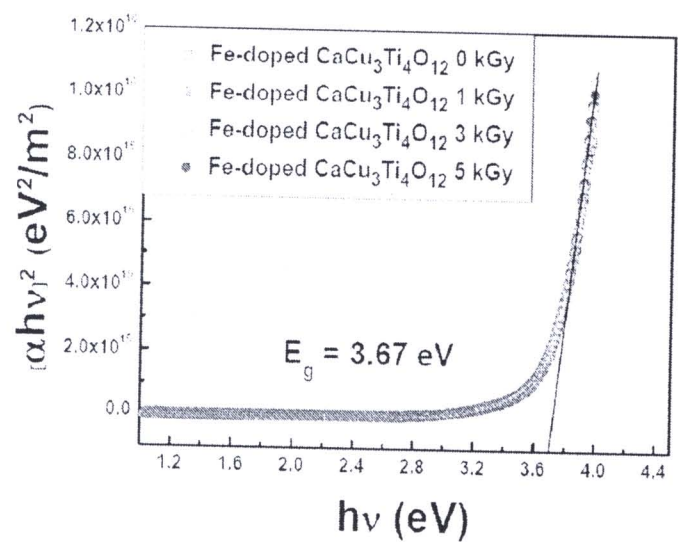


Figure 2. Plot between $(\alpha h\nu)^2$ versus $h\nu$ of Fe-doped $\text{CaCu}_3\text{Ti}_4\text{O}_{12}$ thin films.

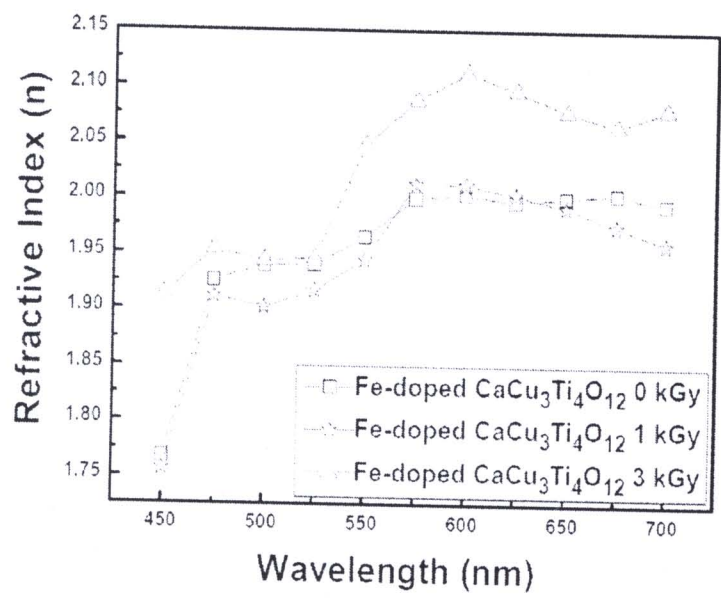


Figure 3. The refractive index of Fe-doped $\text{CaCu}_3\text{Ti}_4\text{O}_{12}$ thin films for different gamma radiation dose.

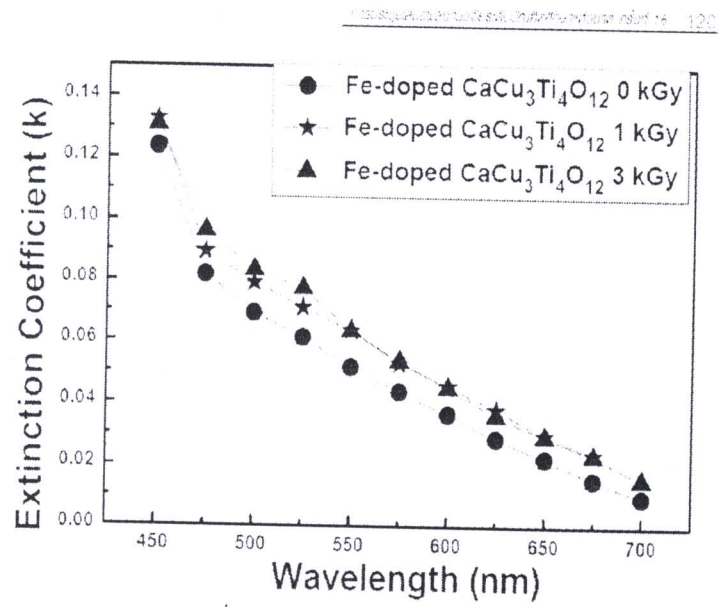


Figure 4 The extinction coefficient of Fe-doped $\text{CaCu}_3\text{Ti}_4\text{O}_{12}$ thin films for different gamma radiation dose

Vitae

Miss. Ornnich Kongwut was born on December 18, 1984 in Kanchanaburi, Thailand. She finished high school from Kanchananukroh, Kanchanaburi in 2002, then received her Bachelor degree of Science in Physics from Mahidol University in 2006, and continued her Masters study in Physics at Chulalongkorn University.



